Collective Resonances in Gold Nanoparticle Arrays

Baptiste Auguié* and William L. Barnes

School of Physics, University of Exeter, Stocker Road, Exeter, Devon, EX4 4QL, United Kingdom

(Received 16 May 2008; revised manuscript received 23 July 2008; published 30 September 2008)

We present experimental evidence of sharp spectral features in the optical response of 2D arrays of gold nanorods. A simple coupled dipole model is used to describe the main features of the observed spectral line shape. The resonance involves an interplay between the excitation of plasmons localized on the particles and diffraction resulting from the scattering by the periodic arrangement of these particles. We investigate this interplay by varying the particle size, aspect ratio, and interparticle spacing, and observe the effect on the position, width, and intensity of the sharp spectral feature.

DOI: 10.1103/PhysRevLett.101.143902 PACS numbers: 42.25.Fx, 73.20.Mf

Nanoparticles of noble metals have been the subject of many detailed studies due to their unique optical properties [1], in particular because they can support localized surface plasmon resonances (LSPR) [2]. The LSPR associated with metal nanoparticles exhibit a high degree of optical field confinement [3,4], together with a high sensitivity to their local environment. Where two or more metallic nanostructures are in close proximity, the possibility exists for interaction between the modes of the individual nanostructures to form new hybrid modes [5]. The case of two interacting particles has been extensively studied (for example, see [6]). For multiple nanostructures there is also the possibility of coherent interaction arising from multiple scattering. Light that is scattered so as to propagate in the plane of the particles will undergo multiple scattering by the regularly spaced particles. A geometric resonance arises when the wavelength of the scattered light is commensurate with the periodicity of the array, which, when it occurs in the same spectral range as the LSPR, may lead to a dramatic modification of the measured optical extinction. It appears that this effect was first predicted by Carron *et al.* (see, for example, [7]) and Markel [8,9] and more recently followed up by Zou *et al.* [10]. Further theoretical or computational work by these groups has extended our understanding [8–13], and a tutorial review linking these concepts to those associated with hole arrays has recently been given [14].

Experiments to confirm the existence of these sharp diffractive features in the optical response of metallic nanoparticle arrays have met with only limited success. Haynes *et al.* [15], Hicks *et al.* [16], Sung *et al.* [17], and Lamprecht *et al.* [18] performed detailed studies of arrays of gold and silver nanoparticles, but the effect was not as pronounced as expected from the modeling. In each case, failure to observe the sharp spectral features appears to be due to one or more of the following factors: lack of an homogeneous environment, an angle spread of the illumination, an inappropriate choice of the particle volume and aspect ratio. Félidj *et al.* [19] reported sharp features in a system consisting of a regular array of gold nanorods supported on a thin indium tin oxide (ITO) layer. However, the presence of the ITO layer complicates the analysis and makes the underlying physics harder to unravel: such a system leads to a rich physics when the ITO is thick enough to support waveguide modes that interact with the LSPR [20]. Here we report measurements from regular arrays of gold nanorods in an homogeneous index environment that exhibit the expected sharp peaks in extinction. The homogeneous environment allows us to apply a simple analytical model and so clarify the physics. Further, we explore the role of array period, particle size, and particle shape on the spectral line shape. First we look at a simple semianalytical model, then we discuss the results of our experiments.

In the coupled dipole approximation, each particle is modeled by a dipole of polarizability α. We summarize here the spirit and notation of Ref. [12] and refer the reader to other references [11,13] for a more complete treatment. The particles studied in this work are described as ellipsoids (semiaxes a, b, and c, volume V), for which the static polarizability can be written as [21]

$$\alpha^{\text{static}} \propto V \frac{\varepsilon_m - \varepsilon_d}{3\varepsilon_m + 3\chi(\varepsilon_m - \varepsilon_d)}, \tag{1}$$

with ε_m and ε_d the relative permittivities of the metal and surrounding medium, respectively, and χ a shape factor. When the particle size is of order 50 nm or more, this expression needs to be modified to account for dynamic depolarization and radiative damping—the modified long wavelength approximation (MLWA) [22]. We do so by introducing an effective polarizability $\alpha^{\text{MLWA}} = \alpha^{\text{static}}/(1 - \frac{2}{3}ik^3\alpha^{\text{static}} - \frac{k^2}{a}\alpha^{\text{static}})$, $k = nk_0$ being the wave number in the (homogeneous) surrounding medium which has refractive index n. When excited by an electromagnetic wave at frequency ω, a dipole reradiates a scattered wave in proportion to its dipole moment. The net field on every dipole is therefore the sum of the incident field plus the radiation from all other dipoles, which leads to a system of coupled equations to be solved self-consistently for the total field. Assuming an infinite array, the general

solution can be expressed as an effective polarizability $\alpha^\star$ for every (indistinguishable) particle,

$$\alpha^\star = \frac{1}{1/\alpha - S}, \tag{2}$$

where the array factor S embraces the contribution from the other dipoles, and is only dependent on geometrical parameters. In the case of normal incidence, and for a square array of dipoles, this factor is

$$S = \sum_{\text{dipoles}} e^{ikr}\left[\frac{(1-ikr)(3\cos^2\theta - 1)}{r^3} + \frac{k^2\sin^2\theta}{r}\right], \tag{3}$$

θ being the in-plane angle between the dipole locations. The poles of the effective polarizability define the resonances [9] and result from an interplay between the particle properties and the geometrical array factor. When the imaginary part of S is negative, a partial cancellation of the radiative damping has been predicted [23], thus improving the quality factor of localized surface plasma resonances. The optical extinction cross section σ_{ext} is obtained from the polarizability using the optical theorem by [11,21], $\sigma_{\text{ext}} \propto k\,\text{Im}(\alpha)$.

Using this simple approach we are able to qualitatively understand the spectral features observed in the experiments. Figure 1 presents an example of this calculation for an isolated gold ellipsoid and for the situation when the ellipsoid is part of a periodic square array. Several features may be noted. (i) A peak in the extinction curve (top panel) is obtained when the real part of $(1/\alpha - S)$ vanishes in Eq. (2) [9]. These crossing points are shown by dot-dashed gray lines. (ii) The jumps in both the real and imaginary part of S (bottom panel) are associated with diffraction: the two vertical dashed red lines indicate the position of the $\langle 1, 0\rangle$ and $\langle 1, 1\rangle$ diffraction edges for this square grating. (iii) The intensity of the resulting extinction peaks (upper panel) depends on the imaginary part of S at this wavelength, and the width will also depend on the slope of both $1/\alpha$ and the real part of S [14]. The inset shows the effect of pitch variation and reveals two different regimes. When the diffraction edge is on the high-energy side of the main LSP resonance ($nh < \lambda_0$), very little radiative coupling can occur as the allowed diffracted orders are all of higher energy than the plasmon resonance. The thin blue curves show the effect of pitch variation in this regime, the spectra show a Fano-type shape resulting from interference between directly transmitted light and light scattered by the array. Notice also that the main resonance is sharpened, redshifted, and enhanced with respect to the isolated LSPR. In the other regime, when the diffraction edge is on the low-energy side of the main resonance ($nh > \lambda_0$, thick red curves), a very sharp and intense peak is found in the long wavelength tail of the main resonance; its intensity and width decrease for peak positions further from the main resonance.

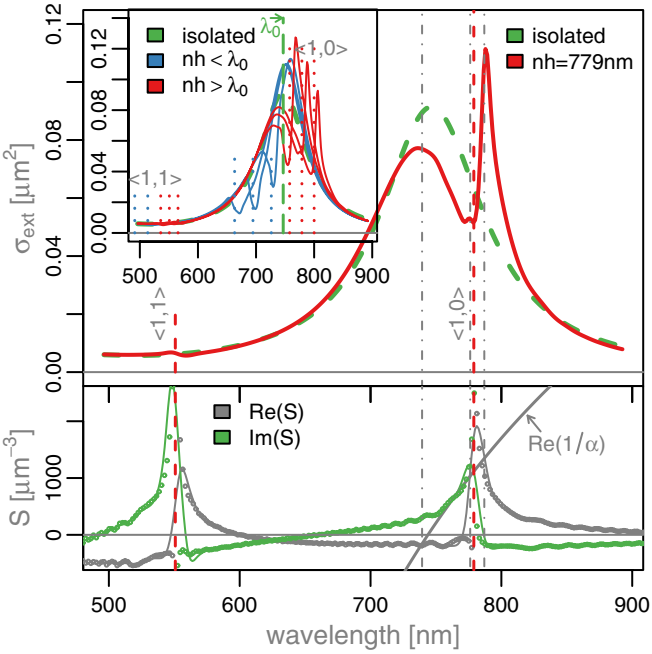

FIG. 1 (color online). Top: Calculated isolated particle extinction cross section for an ellipsoidal particle (semiaxes: $a = 60$ nm, $b = 40$ nm, $c = 15$ nm, surrounding medium: $n = 1.46$, incident light polarized along a). Solid red curve: Same particle in an array. Inset: Effect of pitch variation. The pitch values h are 454, 476, and 497 nm for the thin blue curves and 519, 534, 548 nm for the thick red curves. Bottom: Corresponding calculated array factor (real and imaginary part). The finite number of dipoles (400×400) creates spurious fast oscillations in the array factor S, which were smoothed before insertion in Eq. (3) (continuous lines).

To explore these phenomena, we fabricated and characterized a number of gold nanorod arrays. The samples were produced by electron beam lithography on fused silica substrates ($n = 1.46$). A 100 nm thick layer of poly(methyl methacrylate) (PMMA) resist was spin coated on the substrates, with a 15 nm thick gold overlayer deposited by thermal evaporation to ensure the electrical conductivity required for the electron beam lithography exposure. The spatial extent of the arrays was 35 μm $\times$ 35 μm. Particle sizes were in the range 50—120 nm with aspect ratios ranging from 1:1 to 2:1. This spread of sizes was dictated by three parameters: (i) the spectral range of our acquisition system (400–900 nm), (ii) the requirement that only the dipolar mode contributes substantially to the optical response of the particles, (iii) smaller particles have resonances that suffer from strong absorption by the gold. After developing the exposed resist mask, a 2 nm chromium adhesion layer was deposited by thermal evaporation, followed by a 35 nm thick gold layer (99.99% purity, pressure 2×10^{-6} Torr). We found that this very thin layer of chromium did not alter noticeably the LSPR. The in-plane particle geometries were measured by scanning electron

microscopy (SEM), and the particle height measured by a calibrated crystal monitor during the deposition, and cross-checked by a tilted SEM image. The optical characterization of the sample was undertaken using bright-field transmission spectroscopy at normal incidence (angular spread $<0.1°$), in an index matching index fluid ($n = 1.46$).

Two sets of transmission spectra are shown in Fig. 2 for varying particle separations. The top panel corresponds to a homogeneous (index matched) surrounding environment. Several features are apparent from these curves. (i) As the periodicity is varied, a sharp interference pattern sweeps through a broad resonance (the isolated localized plasmon resonance with a typical width of ~100 nm, centered at ~710 nm). (ii) A clear correlation between the sharp transmission dip and the array pitch exists. The bottom panel presents the equivalent result for an asymmetric index configuration where air replaces the index matching oil. Here, the asymmetry between substrate and superstrate strongly hinders the radiative coupling effect between particles and we observe very similar results to previous experimental studies [18,24]: a strong asymmetry in the spectral line shape, but without the presence of a sharp dip near the diffraction edge. Note that in the homogeneous environment (top panel), a weak secondary minimum is present on the high-energy side of the sharp diffractive feature. Félidj *et al.* observed something similar [19], but for a sample where the particles were supported on a thin ITO layer. Our observation in the absence of index asymmetry suggests that the additional minimum cannot be explained by two diffracting conditions, as suggested in [19]. To further support this argument, we note that the relationship between the two minima and the diffraction edge changes as the diffraction edge sweeps through the particle resonance (more clearly seen in Fig. 3).

Focusing now on the symmetric index configuration that displays a sharp spectral feature, the experimental data were processed as follows. First, the transmittance spectra for different particle separations were scaled to account for the fact that a different number of particles contribute to the extinction. Second, as the transmittance per particle has little physical meaning, it was converted into an extinction cross section, related to the measured transmittance T by $\sigma_{\text{ext}} = h^2(1 - T)$. In this way, we obtain the results plotted in Fig. 3, results that show all the features expected from the coupled dipole model (see inset of Fig. 1). Note that the area under the extinction curve appears to be constant, as suggested by a sum rule for extinction [25].

When studying the sharp feature and its dependency on the different parameters, it is useful to try to decorrelate the effect of particle separation, particle volume, and particle aspect ratio. By using a range of samples so as to give a large spread of particle sizes, we were able to obtain the extinction from two arrays for which particles of different aspect ratio had the same volume. The use of a polarizer allows us to compare the two in-plane axes for a given particle, as shown in Fig. 4. The more elongated particles

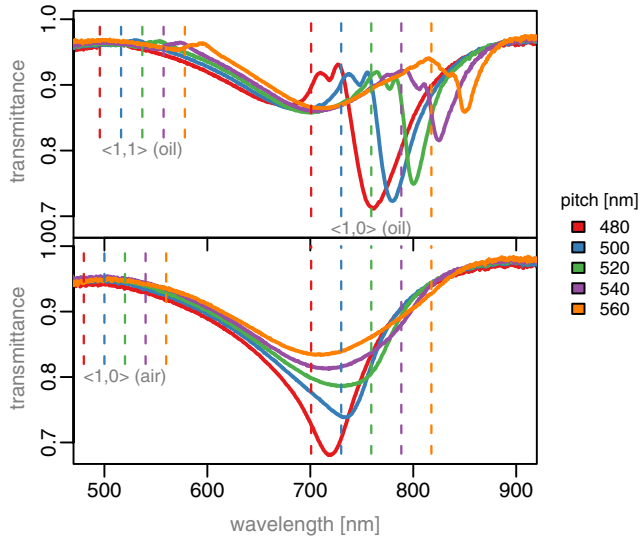

FIG. 2 (color online). Transmittance spectra for gold nanorod arrays in an homogeneous index environment (top, oil immersion $n = 1.46$) and asymmetric refractive index configuration (bottom, incident light in air), for five particle separations. Nominal particle sizes: 100 nm × 90 nm × 35 nm (top), 120 nm × 90 nm × 35 nm (bottom). The vertical lines indicate the position of the $\langle 1, 0\rangle$ and $\langle 1, 1\rangle$ diffraction edges for the two refractive index environment configurations.

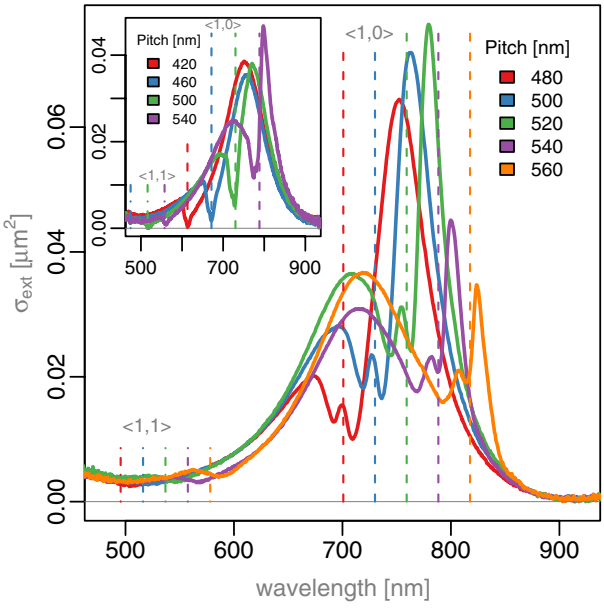

FIG. 3 (color online). Extinction spectra (per particle) for several gold nanoparticle arrays. The average particle size was 123 nm × 85 nm × 35 nm. Inset (nominal particle size 120 nm × 90 nm × 35 nm): When the diffraction edge is on the blue side of the main resonance, a much weaker effect is observed. Interestingly, complete transmission can be obtained near the diffraction edge; see especially the curve for 420 nm pitch in the inset.

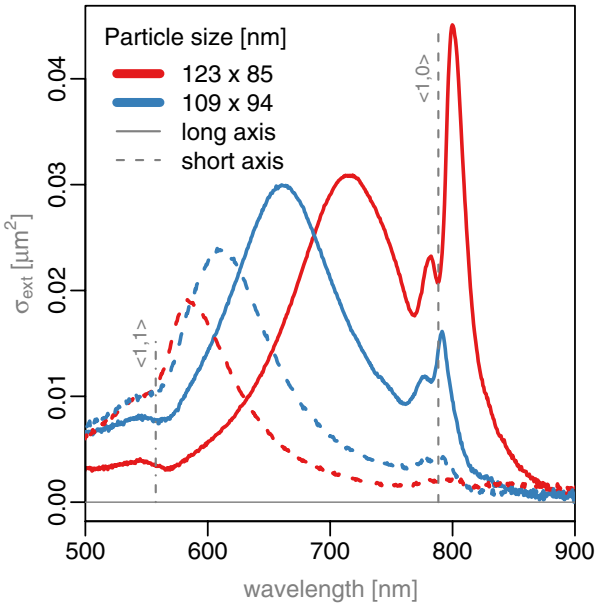

FIG. 4 (color online). Extinction spectra, normalized by the occupancy for two polarization states (long axis: solid lines; short-axis: dashed lines). The colors refer to two arrays of particles both of pitch 540 nm for which the particle volume is approximately the same, but the particles have different aspect ratios.

exhibit a redshifted resonance along the long axis, the short axis being blueshifted. As expected, the particle volume alone is not sufficient to uniquely determine the observed spectral features. In particular, the sharp peak near the diffraction edge is much more intense for the case of the higher aspect ratio particle, at a constant volume and constant particle separation. In these measurements, the peak intensity is mainly dictated by the proximity of the diffraction edge to the LSP resonance, which in turn is determined by the particle polarizability, a function of both the volume and aspect ratio [Eq. (1)]. We expect that the radiative coupling between particles will depend on the overlap between the propagating field and the mode associated with the localized plasmon resonance.

We have shown experimental evidence for the narrow spectral features in the optical response of periodic metal nanoparticle arrays that have been predicted in the literature for several years now. The periodic arrangement of nanorods introduces an interference feature close to the diffraction edge, and its position with respect to the localized plasmon resonance was varied by changing the particle separation.

The authors would like to thank Dr. Sasha Grigorenko for interesting discussions, the anonymous referees for useful suggestions, and the EPSRC (EP/C52389X/1) for funding through the Basic Technology project "2D Attogram Surface Plasmon Resonance Imaging." W. L. B. thanks the Royal Society for financial support.

*ba208@exeter.ac.uk

[1] U. Kreibig and M. Vollmer, *Optical Properties of Metal Clusters* (Springer, Berlin, 1995).
[2] C. Haynes and R. P. Van Duyne, J. Phys. Chem. B **105**, 5599 (2001).
[3] W. A. Murray, J. R. Suckling, and W. L. Barnes, Nano Lett. **6**, 1772 (2006).
[4] A. Whitney, J. Phys. Chem. B **109**, 20522 (2005).
[5] E. Prodan, C. Radlo, N. Halas, and P. Nordlander, Science **302**, 419 (2003).
[6] L. Gunnarsson, T. Rindzevicius, J. Prikulis, B. Kasemo, M. Käll, S. Zou, and G. C. Schatz, J. Phys. Chem. B **109**, 1079 (2005).
[7] K. T. Carron, W. Fluhr, M. Meier, A. Wokaun, and H. W. Lehmann, J. Opt. Soc. Am. B **3**, 430 (1986).
[8] V. A. Markel, J. Mod. Opt. **40**, 2281 (1993).
[9] V. A. Markel, J. Phys. B **38**, L115 (2005).
[10] S. Zou, N. Janel, and G. C. Schatz, J. Chem. Phys. **120**, 10 871 (2004).
[11] S. Zou and G. C. Schatz, J. Chem. Phys. **121**, 12 606 (2004).
[12] S. Zou and G. C. Schatz, Nanotechnology **17**, 2813 (2006).
[13] V. A. Markel and A. Sarychev, Phys. Rev. B **75**, 085426 (2007).
[14] F. J. G. de Abajo, Rev. Mod. Phys. **79**, 1267 (2007).
[15] C. Haynes, A. McFarland, L. L. Zhao, R. P. VanDuyne, G. C. Schatz, L. Gunnarsson, J. Prikulis, B. Kasemo, and M. Käll, J. Phys. Chem. B **107**, 7337 (2003).
[16] E. M. Hicks, S. Zou, G. C. Schatz, K. G. Spears, R. P. Van Duyne, L. Gunnarsson, T. Rindzevicius, B. Kasemo, and M. Käll, Nano Lett. **5**, 1065 (2005).
[17] J. Sung, E. M. Hicks, R. P. Van Duyne, and K. G. Spears, J. Phys. Chem. C **112**, 4091 (2008).
[18] B. Lamprecht, G. Schider, R. Lechner, H. Ditlbacher, J. Krenn, A. Leitner, and F. Aussenegg, Phys. Rev. Lett. **84**, 4721 (2000).
[19] N. Félidj, G. Laurent, J. Aubard, G. Levi, A. Hohenau, J. Krenn, and F. Aussenegg, J. Chem. Phys. **123**, 221103 (2005).
[20] S. Linden, J. Kuhl, and H. Giessen, Phys. Rev. Lett. **86**, 4688 (2001).
[21] C. Bohren and D. Huffman, *Absorption and Scattering of Light by Small Particles* (John Wiley & Sons, New York, 1983).
[22] T. Jensen, K. L. Kelly, A. Lazarides, and G. C. Schatz, J. Cluster Sci. **10**, 295 (1999).
[23] S. Zou and G. C. Schatz, J. Chem. Phys. **122**, 097102 (2005).
[24] A. Hohenau, J. R. Krenn, S. G. Rodrigo, L. Martin-Moreno, and F. Garcia-Vidal, Phys. Rev. B **73**, 155404 (2006).
[25] E. Purcell, Astrophys. J. **158**, 433 (1969).